5 October 1998

PHYSICS LETTERS A

ELSEVIER

Physics Letters A 247 (1998) 119–128

Impulse control of chaos in continuous systems

G.V. Osipov [a,b], A.K. Kozlov [c], V.D. Shalfeev [a]

[a] *Department of Radiophysics, University of Nizhny Novgorod, 23 Gagarin Ave., Nizhny Novgorod 603600, Russia*

[b] *Department of Biomedical Engineering, Boston University, 44 Cummington Street, Boston, MA 02215, USA*

[c] *Institute of Applied Physics, Russian Academy of Science, 46 Uljanov Street, Nizhny Novgorod 603600, Russia*

Received 4 November 1997; revised manuscript received 20 April 1998; accepted for publication 6 July 1998
Communicated by A.P. Fordy

Abstract

Several methods of nonconstant feedback impulse control of chaos are proposed. The approach is based on the similarity of the return maps of dissipative continuous-time systems with one-dimensional maps and has a clear geometrical interpretation. The methods are illustrated for Chua's circuit, the Rössler oscillator, and the phase-locked loop system. © 1998 Elsevier Science B.V.

1. Introduction

The dynamic chaos encountered in many physical and engineering problems is an undesirable effect leading to irregular and unpredictable behavior. At the same time, chaos is a typical phenomenon in nonlinear dynamic systems whose phase space has a dimension not lower than three. In this connection there arise two basic questions:

(i) Under what conditions does chaotic motion occur?

(ii) How can chaotic motion be controlled?

The first question involves the investigation of the position of the existence domain of chaotic motions in the parameter space of a dynamic system. This is one of the fundamental problems in nonlinear dynamics. Numerous researches were attempted in this field for various objects in the past thirty years [1–3]. The ways the dynamic chaos appears may, in general terms, be regarded to be a solved problem.

The problem of controlling chaotic behavior of dynamic systems has received proper attention only in recent years [4–6]. We can say that controlling chaos became possible after the geometry of chaotic attractors had been understood. This explains, in part, that a significant advance was made in controlling chaos in low-dimensional systems. In particular, some methods were elaborated that allow one to realize a controlled transition from chaotic to regular oscillations in a specific dynamic system. Today, the following methods of controlling chaotic behavior are available:

(i) search for and stabilization of unstable periodic motion "contained" in the chaotic set [7–9];

(ii) suppression of chaotic behavior by external forcing: periodic [10–13], noise [10], periodic parametric perturbation [10,14];

(iii) algorithms of automatic control, including adaptive control [15–18].

These may be applied in two ways that give the same result, namely, a change of attractor in the system. The first type of control includes methods of parametric control, i.e., when one or several parameters of the system are changed employing a certain strategy. In this case, we can speak about control by means of

PII S0375-9601(98)00536-2

systemparameter(s). This type of control is reasonable when the variation of parameters of the object can readily be achieved, for example, in different electrical and radio engineering systems. For the second type of control we refer to methods where one can change the position of the point in the phase space of the system at constant values of its parameters. Such a control is rendered possible by adding to the system a new parameter (or several such parameters) that may be regarded as a control. This is the only possible method for controlling the behavior of a chaotic system when the system parameters cannot be changed.

In a general case, the control by means of changing a system or a control parameter reduces to finding the perturbation u that would allow for passing from chaotic to regular behavior in the system.

In this paper, we propose several procedures for controlling chaotic dynamics of continuous-time systems described by ordinary differential equations by *impulse* variation of control parameter (see also Refs. [19,20]). Being rather specific, these control methods consist, basically, of suppressing chaos in the return map generated by the trajectories of the continuous system at the Poincaré section. Impulse control of continuous dynamic systems has been attracting great attention [21,22] mainly because of the need to solve specific problems that are encountered in applying time-discrete maps to continuous systems. The use of impulse forcing may enable one to achieve control in a much simpler way and, in some cases, even to obtain an exact analytical solution of the problem [21].

Let us formulate the procedure of suppressing chaotic oscillations by changing the control parameter on the example of a return map generating chaos. We consider control in chaotic continuous systems giving one-dimensional maps. We take a chaotic map

$$x_{n+1} = F(x_n)\,. \tag{1}$$

We need to find for the continuous system the impulse control $e(t) = E(x(t), t)$ such that the resulting map

$$x_{n+1} = F(x_n) + u_n, \quad u_{n+1} = G(x_n, u_n)\,, \tag{2}$$

where $u_n = u(E)$, should produce a regular trajectory. Control of the continuous system dynamics is accomplished by means of (i) constant duration and amplitude impulses that do not depend on the current state of the system for the Poincaré section and give the control law $G(x_n, u_n) = u_n$ in the map (2); (ii) constant duration and amplitude impulses for which the conditions of feeding depend on the current state of the system for the Poincaré section, i.e., the function $G(x_n, u_n) = u_n + G^*(x_n)$ in (2); and (iii) the impulses whose amplitude, duration and conditions of feeding obey a certain known law of control. Each of the procedures proposed is described in a separate section, where its application is demonstrated first for a model return map and then for a concrete continuous system. The specific feature of the methods described in the two first sections is that chaos is controlled not by stabilizing unstable limit cycles of chaotic manifolds, as is the case of controlling chaos on a Poincaré section [7], but by generating a new stable periodic solution. Consequently, there is no need to carry out a preliminary analysis of the system under consideration, for example, to determine coordinates and eigenvectors of the periodic motion to be stabilized, as in the method of Ott, Grebogi, and Yorke (OGY) [7]. The system to which an external impulse force is applied may be regarded as a "black box" generating a one-dimensional chaotic map. At the same time, given known equations for dynamic system, the magnitude of the controlled force may be determined analytically from the solution of the linearized problem.

The procedure of automatic impulse control proposed in Section 3 is based on one of the methods of the classical theory of control. A saddle periodic solution embedded in a chaotic attractor is stabilized by means of an adaptive small-magnitude force.

Note also that the novelty of our approach is that we focus attention on the geometrical interpretation of the method of adaptive impulse control.

As was mentioned above, the necessary condition for using the proposed control strategy is the contingency to describe, at least approximately, the behavior of the continuous system through a one-dimensional return map. This is usually possible in continuous systems with strong dissipation. Such systems are Chua's circuit, the Rössler oscillator and the phase-locked loop (PLL) that are used as examples in which chaotic oscillations are suppressed.

2. Chaos suppression by constant impulses

2.1. Map shift

Let us demonstrate the transition from a chaotic to a regular regime for a one-dimensional map of the square type.

Evidently, the simplest way to obtain a fixed point for the map (1) producing chaos is to shift this map upwards or downwards [23], so that the local slope of the map function at the new fixed point x^* would satisfy the stability condition $|dF(x)/dx|_{x^*} < 1$ as shown in Fig. 1. For the square function F, the transition from chaos to a stable fixed point may be accomplished by means of a constant shift: $x_{n+1} = F(x_n) + u_n$ for $u_n = u^*$. In addition, by choosing the control magnitude u^* one can obtain stable periodic orbits of needed periods. Using this method we will show how chaos in Chua's circuit may be suppressed by impulse forcing.

2.2. Controlling Chua's circuit

Chua's circuit is an electronic scheme consisting of one nonlinear and four linear elements and is described by a set of differential equations [24],

$$\dot{x} = \alpha(y - x - f(x)), \quad \dot{y} = x - y + z,$$
$$\dot{z} = -\beta y, \tag{3}$$

where $f(x)$ is a piecewise linear function

$$\begin{aligned} f(x) &= bx - (a-b), && x \leqslant -1, \\ &= ax, && |x| < 1, \\ &= bx + (a-b), && x \geqslant 1. \end{aligned} \tag{4}$$

All the computations were carried out for the values of the parameters $\alpha = 8.72, \beta = 14.29, a = -8/7$, and $b = -5/7$ and the initial conditions $x(0) = 0.1, y(0) = 0$, and $z(0) = -0.1$.

It is well known [24] that, as the parameter α grows in Chua's circuit, two spiral chaotic attractors arise in the system through cascades of period doubling bifurcations of symmetric periodic motions. One of these attractors is located entirely in the region $x > 0$, and the other in the region $x < 0$. Consider the spiral chaotic attractor in the region $x > 0$. Fig. 2 shows the return map for this attractor: $x_{n+1} = F(x_n)$, where x_n is the value of the x-coordinate of the chaotic tra-

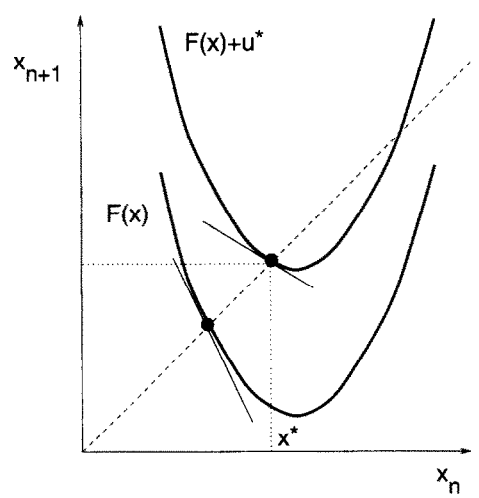

Fig. 1. Obtaining stable fixed point x^* using the map shift by u^*.

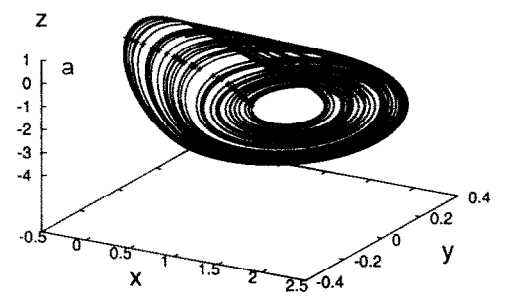

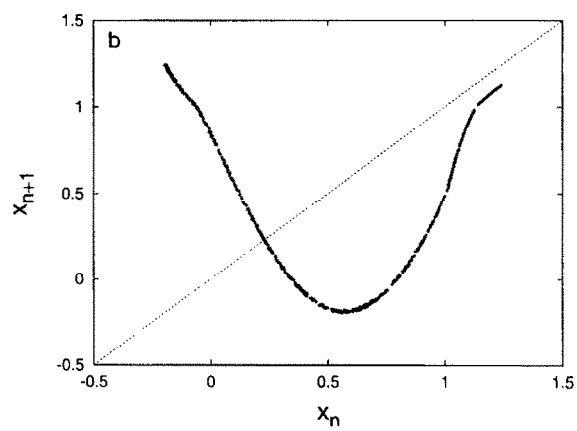

Fig. 2. Chaotic attractor from Chua's circuit: (a) trajectory of the continuous system; (b) one-dimensional Poincaré map induced by intersections of the trajectory with the cross section $y = -0.1$.

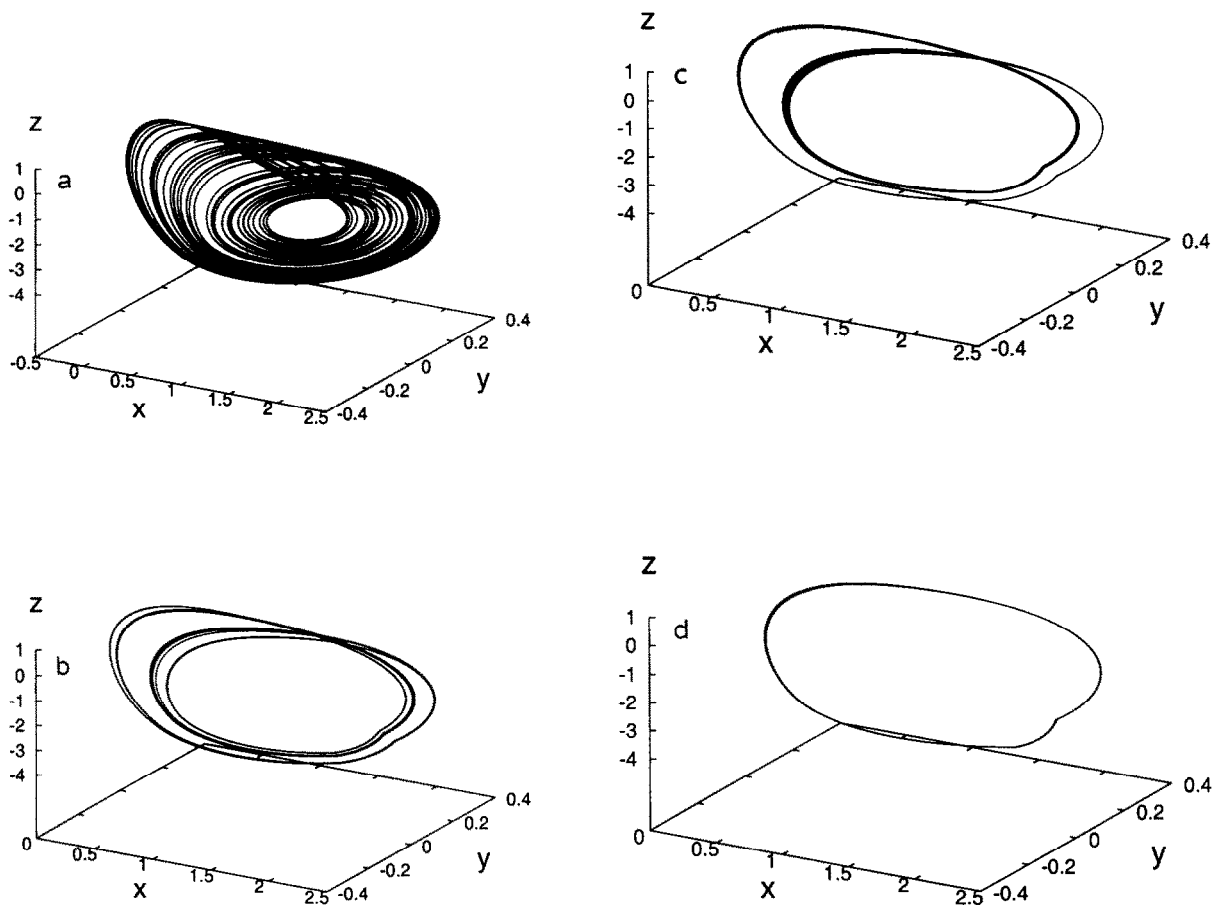

Fig. 3. Controlling Chua's circuit to periodic orbits by an impulse force of constant impulse magnitude E_0: (a) $E_0 = 0$, no control; (b) $E_0 = 1.2$; (c) $E_0 = 1.4$; (d) $E_0 = 2.1$.

jectory at the intersection with the plane $y = -0.1$. It is clear from Fig. 2 that the map has a square shape, which is typical of the return maps depicting the evolution of chaos through a cascade of period doubling bifurcations. For suppression of chaotic oscillations in Chua's circuit by controlling, the map must be shifted upwards by a certain value so that a stable cycle should appear (Fig. 1). This can be attained by adding as a control term an external impulse force $e(t)$ to the first equation of the system (3),

$$\dot{x} = \alpha(y - x - f(x)) + e(t), \quad \dot{y} = x - y + z,$$
$$\dot{z} = -\beta y, \tag{5}$$

where

$$e(t) \equiv E(x(t),$$
$$y(t)) = E_0, \quad t \in \Delta t,$$
$$= 0, \quad t \notin \Delta t. \tag{6}$$

In the case of interest, the value of the interval Δt is determined by the time the phase trajectory remains inside the region $|y| < \varepsilon = 0.1, x < 1.5$. In other words, the procedure of suppressing chaos in Chua's circuit reduces to feeding an external impulse force of constant magnitude E_0 while the point is staying in the ε-neighborhood of the $y = 0$ plane at $x < 1.5$. Note that, since the external forcing is fed exclusively in the region of linearity of the system considered, it is obvious that the dependence $u_n(E)$ may be determined analytically. The cycles of periods 4, 2 and 1 depicted in Fig. 3 are observed for $E_0 = 1.2, 1.4$, and

2.1, respectively.

3. "Local" impulse control

In the previous section, we described the method of suppressing chaos that leads to changes in the Poincaré map for one of the variables of the system throughout its range of variations D. In other words, we fed an external pulsed force every time the point was inside a certain neighborhood of the secant plane. Numerical experiments show, however, that the number of fed impulses and, consequently, the energy consumption on suppressing chaos may be diminished significantly by transforming the map F describing the chaotic behavior of the system not for the whole region of variation D of some variable, but only on a certain interval l. We will show below that the size of this interval l may be small (not greater than 5% of the size of the region D in this section). Hereafter, we will refer to this method of chaos suppression as "local" impulse control.

3.1. Local perturbation of the map

We first demonstrate suppression of chaos by local impulse control on the example of a model return map,

$$\begin{aligned} x_{n+1} &= |1 - 2x_n|, \quad b \leqslant x_n \leqslant 1, \\ &= 1 - 2b, \qquad 0 \leqslant x_n \leqslant b, \end{aligned} \tag{7}$$

where the parameter b is responsible for control. In the absence of forcing ($b = 0$), the map (7) produces a chaotic trajectory. This piecewise linear map may be investigated analytically. Periodic orbits of small periods are found relatively easily. The stability of an arbitrary periodic orbit $x_1, x_2, \ldots, x_k$ is determined by the product $P = |f(x_1)||f(x_2)| \ldots |f(x_k)|$. In our case, the condition $|f(x_j)| = 0$ is fulfilled for an arbitrary point x_j from the set $x_1, x_2, \ldots, x_k$ belonging to the interval $[0, b]$. Consequently, any periodic trajectory produced by the map (7) at $b \neq 0$ and having as one of the coordinates, at least, a point belonging to the interval $[0, b]$ is stable because $P = 0$ for it. We obtained a bifurcation diagram characterizing the evolution of the trajectories realized in the map (7) depending on the magnitude of the parameter b. As b is increased, the chaotic motion existing at $b = 0$ undergoes a cascade of bifurcations, which eventually leads to emergence of a stable fixed point at $b = 1/3$.

Chaos suppression may proceed as follows. Suppose that we choose a periodic orbit (and the corresponding value of parameter b) which we want to obtain as a result of control. Then, in the course of map iteration, as soon as the current value of the x_n-coordinate gets into the interval $[0, b]$, the value $u = -2(x_n - b)$ is subtracted from x_{n+1}. After that, we get to a stable orbit of a given period only in one iteration. Examples of impulse implementation of this method for continuous systems are given in Subsection 3.2 for fixed u and in Subsection 3.3 for linear controller.

Naturally, transformation of the Poincaré map is more complicated in a real dynamic system than in the model map (7). However, the main idea of local impulse control also proves to be fruitful.

3.2. Controlling the Rössler oscillator

Let us show how the method of local impulse control may be used in a continuous-time system, namely, the Rössler oscillator modeled by a system of ordinary differential equations

$$\begin{aligned} &\dot{x} = -y - z, \quad \dot{y} = x + ay, \\ &\dot{z} = 0.4 + (x - 8.5)z\,. \end{aligned} \tag{8}$$

As the parameter a is increased in the Rössler oscillator, a chaotic attractor appears through a cascade of period doubling bifurcations of periodic motions. We consider the behavior of the system (8) for $a = 0.15$ and $a = 0.18$. A spiral type chaotic attractor is realized in the system at these values of a. If we take as a Poincaré section a half-plane $x = 0$ for $y < 0$, then we can plot a return map $y_{n+1} = F(y_n)$ as a square parabola, that is analogous to the return map for Chua's circuit (Fig. 2b). The region of permissible changes of the variable y is $D_y \simeq [-13, -6]$. Analogously to the procedure of chaos suppression for the model map (7) described in the previous section, we transform the Poincaré map $y_{n+1} = F(y_n)$ for the Rössler system by shifting downwards its portion for the values of y_{n+1} near the left boundary of the region D_y. This can be done by including as control the external impulse force $e(t)$ into the second equation of the system (8),

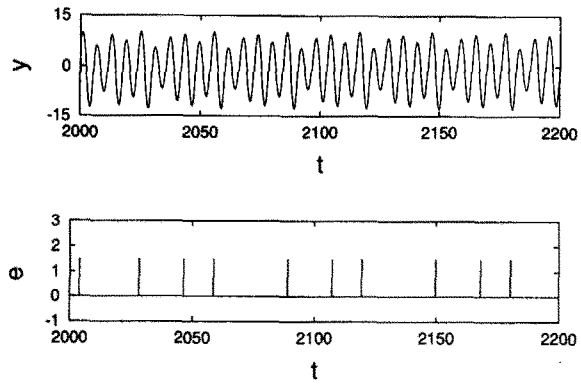

Fig. 4. Suppressing chaos in the Rössler oscillator: (a) time series $y(t)$; (b) impulse time series $e(t)$.

$$\dot{x} = -y - z, \quad \dot{y} = x + ay + e(t),$$
$$\dot{z} = 0.4 + (x - 8.5)z, \tag{9}$$

where

$$e(t) \equiv E(x(t),$$

$$y(t)) = E_0, \quad t \in \Delta t,$$
$$= 0, \quad t \notin \Delta t. \tag{10}$$

Here, the value of the interval Δt is determined by the time the phase trajectory remains inside the small portion of D_y.

The approximate magnitude of the fed impulse needed to change the map F may be calculated by computational runs, i.e., by registering the magnitudes of the system's response to the external impulse forcing depending on the amplitude and duration of the impulse. In some instances (for example, if the force is fed to a relatively short portion of the trajectory), one can make use of the estimates for the magnitude of response to the impulse of a linearized system. An example of chaos suppression in the Rössler system by feeding the external impulse force $E_0 = 1.5$, while the phase point is staying inside the region $|x| < 0.5$, $y < -12$, is given in Fig. 4. As a result, a periodic trajectory of period 5 is realized in the system.

Analogous results of chaos suppression have been obtained by considering the Poincaré map $x_{n+1} = F(x_n)$ at the cross section $y = 0$ for $x < 0$. Our numerical experiments verified that for the map $x_{n+1} = F(x_n)$, the decrease in x_{n+1} near the left boundary of the region of permissible changes of the variable D_x leads to the increase of the values of x_{n+1} near the right boundary. Knowing this fact, we performed a series of experiments in which by means of an external impulse force fed in the region $|y| < 0.5$, $-5 < x < 0$ we suppressed chaos and realized periodic motions. The results are shown in Fig. 5.

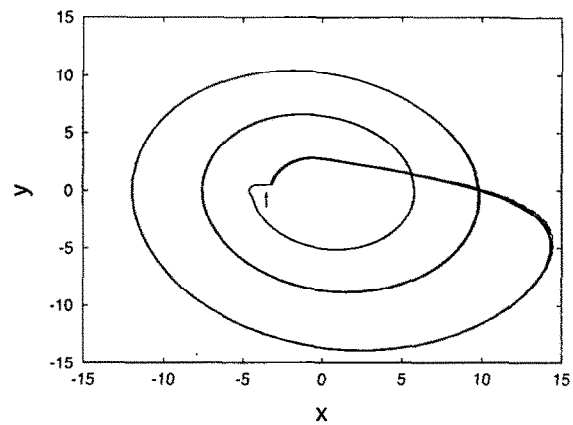

Fig. 5. Periodic trajectory of period 3 obtained by local impulse control. Impulse localization is depicted by the arrow.

The methods of impulse control proposed in Ref. [21] give similar effects of chaos suppression.

4. Automatic impulse control

It was shown above that fixed-magnitude impulse forcing of a continuous dynamic system may give rise to perturbations in the structure of the phase space and attracting set and, thus, generate stable regular regimes. The resulting periodic solution is not the solution of the initial unperturbed system. Numerical experiments on different systems revealed that the magnitude of attractor perturbation (the shift of the one-dimensional map corresponding to it in the simplest case) is proportional to the magnitude of the fed impulses, and the linear dependence holds in a broad range of impulse magnitudes. This property enables one to control the magnitudes of attractor perturbations, i.e., to control the state of the system in phase space, whereas the linear dependence on impulse amplitude provides a simple implementation of control systems. If the obtained stable periodic solution is a

solution of an unperturbed system, then one can say that the periodic orbit *is stabilized* in the chaotic attractor. Below, we consider two methods of impulse local stabilization of a saddle periodic solution inside a chaotic attractor in a continuous nonautonomous PLL model.

4.1. Stabilization of a fixed point of a one-dimensional map by adaptive impulse control

Consider a control system intended for stabilization of a fixed point x^* of the map (1) in the form (2).

For construction of the control law we use the speed-gradient algorithm from the theory of adaptive control [25]. Let us formulate its key points for maps of the general form,

$$\boldsymbol{x}_{n+1} = \mathbf{F}(\boldsymbol{x}_n, \boldsymbol{u}_n)\,,$$

where $\boldsymbol{x}_n = (x_n^{(1)}, \ldots, x_n^{(l)})^T$ is the state vector of the control object, $\boldsymbol{u}_n = (u_n^{(1)}, \ldots, u_n^{(m)})^T$ is the vector of adjusted parameters (control), and $\mathbf{F}(\boldsymbol{x}_n, \boldsymbol{u}_n)$ is the l-dimensional vector function continuously differentiated with respect to $\boldsymbol{x}_n, \boldsymbol{u}_n$. Let $\boldsymbol{x}^*$ be the target state of the system and $Q(\boldsymbol{x}_n, \boldsymbol{x}^*)$ be the target functional ($Q(\boldsymbol{x}_n, \boldsymbol{x}^*) \geqslant 0$, $Q(\boldsymbol{x}^*, \boldsymbol{x}^*) = 0$), for example, the local functional of the form

$$Q(\boldsymbol{x}_n, \boldsymbol{x}^*) = \tfrac{1}{2}[\boldsymbol{x}_n - \boldsymbol{x}^*]^T \mathbf{C}[\boldsymbol{x}_n - \boldsymbol{x}^*]\,,$$

where $\mathbf{C}$ is the $l \times l$-matrix. Then, in the neighborhood of the target $\boldsymbol{x}^*$, the control law has the form

$$\boldsymbol{u}_{n+1} = \boldsymbol{u}_n - \hat{\Gamma} \cdot \operatorname{grad}_{\boldsymbol{u}_n} \omega(\boldsymbol{x}_n, \boldsymbol{u}_n)\,, \tag{11}$$

where $\hat{\Gamma}$ is the $m \times m$-matrix and $\omega(\boldsymbol{x}_n, \boldsymbol{u}_n)$ is the change of the value of the target functional in one iteration of the map ("speed" of variation),

$$\begin{aligned}\omega(\boldsymbol{x}_n, \boldsymbol{u}_n) &= Q(\boldsymbol{x}_{n+1}, \boldsymbol{x}^*) - Q(\boldsymbol{x}_n, \boldsymbol{x}^*) \\ &= Q(\mathbf{F}(\boldsymbol{x}_n) + \boldsymbol{u}_n, \boldsymbol{x}^*) - Q(\boldsymbol{x}_n, \boldsymbol{x}^*)\,.\end{aligned}$$

Unlike the target functional $Q(\boldsymbol{x}_n, \boldsymbol{x}^*)$, the speed $\omega(\boldsymbol{x}_n, \boldsymbol{u}_n)$ depends explicitly on control $\boldsymbol{u}_n$, which allows us straightforward to write a gradient law of control (11). The control law (11) corresponds to a decrease in the *speed* of variation of the target functional to negative values, thus providing diminution of the target functional $Q(\boldsymbol{x}_n, \boldsymbol{x}^*)$.

By applying the speed-gradient algorithm to the smooth one-dimensional map (1) and choosing a local target functional in the form

$$Q(x_n, x^*) = (x_n - x^*)^2\,,$$

we obtain a control system of the form (2) with control nonlinearity

$$G(x_n, u_n) = -2\Gamma(F(x_n) - x^*) + (1 - 2\Gamma)u_n\,, \tag{12}$$

where Γ is the parameter. Note that, if x^* is a fixed point of the map (1), then $G(x^*, 0) = 0$ and $(x^*, 0)$ is the fixed point of the control system (2). The presence of a zero second coordinate at the fixed point $(x^*, 0)$ means that, as the trajectory is approaching the control target, the magnitude of the control signal tends to zero, i.e., stabilization of the fixed point is achieved by a *small signal.*

Let us find the stability conditions for the fixed point $(x^*, 0)$. Rewrite the control system (2) in the form

$$\begin{aligned}x_{n+1} &= F(x_n) + u_n, \\ u_{n+1} &= G(x_n, u_n) = u_n - H(x_n - x^*, u_n)\,,\end{aligned} \tag{13}$$

where x^* is the fixed point of the map (1) and G and H are the smooth functions satisfying the condition

$$G(x^*, 0) = H(0, 0) = 0\,. \tag{14}$$

When the condition (14) is fulfilled, $(x^*, 0)$ is the fixed point of the map (13). The point $(x^*, 0)$ is stable if the eigenvalues $\lambda_{1,2}$ of the Jacobian of the map (13) lie inside the unit circle, namely, for

$$\begin{aligned}&\beta > (k-1)\delta\,, \quad \beta > (1+k)\delta - 2(1+k)\,, \\ &\beta < k\delta + 1 - k\,,\end{aligned} \tag{15}$$

where $k = F'(x^*)$, $\beta = H'_x(0,0) = G'_x(x^*, 0)$, and $\delta = H'_u(0,0) = 1 - G'_u(x^*, 0)$. The fixed point $(x^*, 0)$ is rough inside the region (15). Consequently, the stabilization effect is structurally stable relative to small parameter variations, which allows us to specify the values of all parameters approximately.

Thus, *weak feedback control* may be used to stabilize the unstable fixed points of one-dimensional maps of the form (1), including those possessing chaotic dynamics, independent of the form of the function $F(x)$. The only information one needs to have about the map is the coordinate of the fixed point x^* and

the value of the derivative $k = F'(x^*)$. The parameters $\beta = H'_x(0,0)$ and $\delta = H'_u(0,0)$ of the control law must satisfy the conditions (15) that guarantee local stability of the fixed point $(x^*, 0)$. The choice of the form of the nonlinear function $G(x_n, u_n) = u_n - H(x_n - x^*, u_n)$ depends on the specific requirements placed on the control system (13). It is worthy noting that the nonlinearity of the form (12), also proposed in Ref. [18], that is obtained by the speed-gradient algorithm for the simplest local target functional $Q(x_n, u_n) = (x_n - x^*)^2$, is not the only possible one. For example, the function $H(x_n - x^*, u_n)$ of the form

$$H(x_n - x^*, u_n) = \frac{\beta(x_n - x^*)}{1 + [(x_n - x^*)/0.2]^{10}} + \frac{(\delta - 0.2)u_n}{1 + (u_n/0.2)^{10}} + 0.2u_n \tag{16}$$

also affects local stabilization of the fixed point $(x^*, 0)$ of the map (13) and provides a decrease of the control signal $|u_n|$ at large deviations $|x_n - x^*|$ and $|u_n|$.

4.2. Controlling chaos in a PLL system

Let us employ the control algorithm described above for the problem of impulse stabilization of a periodic solution in a continuous model of a nonautonomous phase-locked loop system,

$$\dot{x} = y, \quad \dot{y} = \gamma - \sin x - (\lambda - \tau\cos x)y + \mu\sin\omega t, \tag{17}$$

where t is the time, x, y designate the phase variables, and $\gamma, \lambda, \tau, \mu, \omega$ are the parameters. For the parameter values

$$\gamma = 0.5, \quad \lambda = 1.01, \quad \tau = 1, \quad \mu = 1, \quad \omega = 1, \tag{18}$$

the system (17) has an asymptotically stable chaotic attractor [26] without rotation along the x-coordinate: $|x(t)| < \pi$. The one-dimensional map generated by the trajectories $(x(t), y(t))$ on this attractor is shown in Fig. 6a. Here, $x_n = x(t_n)$, where $t_n = Tn$, $T = 2\pi/\omega$, $n = 0, 1, 2, \ldots$

We control the system (17) by periodic rectangular impulses

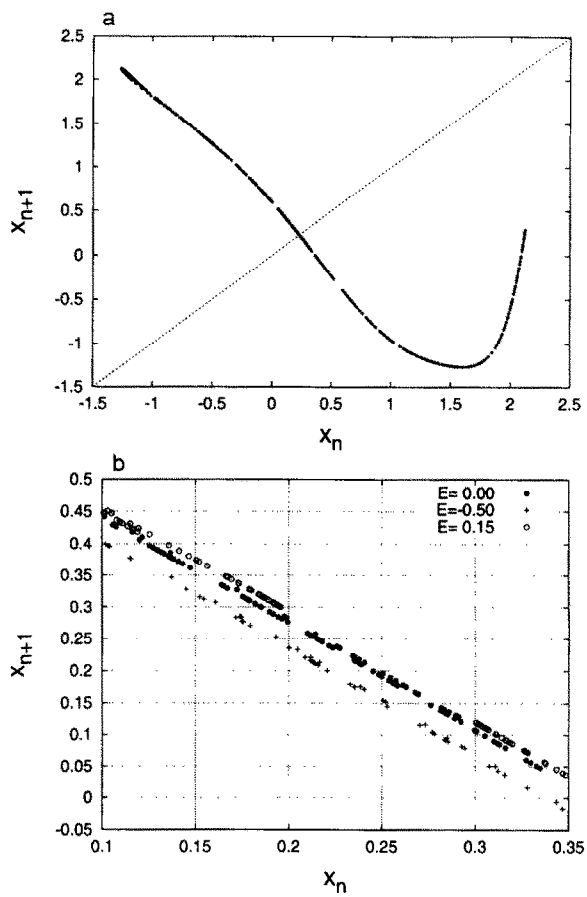

Fig. 6. Shifting one-dimensional map in the continuous-time model of the PLL system by impulse control: (a) original map; (b) maps in the vicinity of the fixed point $x^* \simeq 0.23$ obtained for different impulse magnitudes E.

$$e(t) = -E, \quad t\,(\mathrm{mod}\,T) \in (T - 0.1; T), \qquad = 0, \quad t\,(\mathrm{mod}\,T) \in [0; T - 0.1],$$

adding $e(t)$ to the right-hand side of the second equation of the system (17). Such a perturbation leads to the shift of the map (1) by $u(E)$. The trajectories of the map are depicted in Fig. 6b for different values of impulses E. One can see from Fig. 6b that the shift of the map is proportional to the magnitude of the impulses: $u(E) \simeq \varepsilon E$. By controlling the magnitude of impulses by means of coordinate feedback according to the law

$$E_{n+1} = E_n - \frac{1}{\varepsilon}G(x_n - x^*, \varepsilon E_n), \tag{19}$$

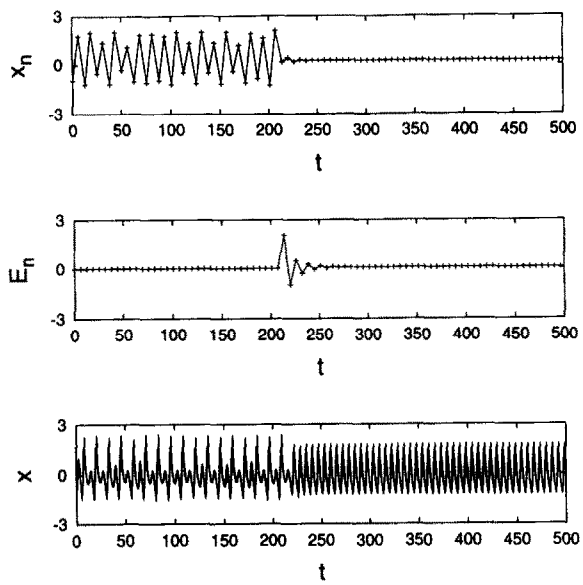

Fig. 7. Stabilizing periodic orbit in the PLL system by adaptive impulse control (x_n is the Poincaré map time series produced by $x(t)$, E_n is impulse time series).

we obtain the control scheme (13) for the continuous system (17). In particular, for the parameter values (18), we have $x^* \simeq 0.23$, $k = F'(x^*) \simeq -1.7$, and $\varepsilon \simeq 0.1$. By choosing the control nonlinearity in the form (16) and the parameters δ, β from the region (15): $\delta = -0.1$, $\beta = 2$, we are able to stabilize the saddle periodic solution of the system (17), that corresponds to the unstable fixed point $x^* \simeq 0.23$ (see Fig. 7).

4.3. Linear controller

When the fixed point of the map (1) is stabilized following the procedure described above, the duration of the transition from the initial state on the attractor to the control target (the neighborhood of the fixed point) depends on the eigenvalues of the matrix of linearized map. But great importance is frequently attached to the speed of the control system. Consider as an example impulse implementation, within the continuous system (17), of the controller that transforms the orbit of a linear map into a fixed point in one iteration.

Let us linearize the map (1) in the neighborhood of the fixed point x^*,

$$x_{n+1} = k(x_n - x^*) + x^*, \tag{20}$$

where $k = F'(x^*)$. Let at some iteration $k = M$ the point x_M be in the neighborhood of x^*. Then, with (20) taken into account, there exists a value of the control signal u_M at which x_M is transformed into x^* in one iteration,

$$u_M = -k(x_M - x^*).$$

For the continuous system (17) with additive impulse control, stabilization of the periodic solution is attained in the second equation

$$\begin{aligned} e(t) = -E_n, \quad & t\,(\mathrm{mod}\,T) \in (T - 0.1; T) \\ & \text{and } |x_n - x^*| < 0.1, \\ = 0, \quad & \text{otherwise} \end{aligned}$$

for the parameter values (18) at the impulse magnitude

$$E_n = \frac{1}{\varepsilon} u_n = -\frac{1}{\varepsilon} k(x_n - x^*), \tag{21}$$

where $x^* \simeq 0.23$, $k \simeq -1.7$, and $\varepsilon = 0.2$. In contrast to the linear case (20), the control target in the continuous nonlinear system (17) is usually not reached in one step, and the control impulses of (21) are fed in each iteration with the number $n \geqslant M$ until the control target is achieved. Nevertheless, it is clear from Fig. 8 that the linear controller (20) may have a rather effective speed in application to the continuous system (17) with impulse control.

5. Conclusion

The methods of controlling chaotic oscillations in continuous dynamic systems described above enable one to pass to periodic oscillations. This is attained by a special control in the form of *additive* impulse forcing that may be realized by three different methods: control by means of the impulses of constant duration and amplitude that are independent of (i) or dependent on the current state of the system (ii), and control by the impulses whose amplitude, duration and the conditions of feeding obey a definite known law of control (iii). The proposed procedures of control are easily realized and are based on a vivid effect of the shift of a one-dimensional map generated by the trajectories

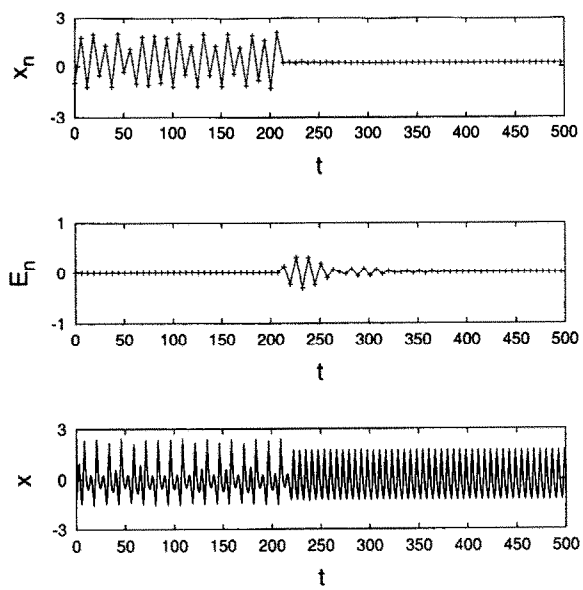

Fig. 8. Stabilizing periodic orbit in the PLL system by linear impulse controller (x_n is the Poincaré map time series produced by $x(t)$, E_n is impulse time series).

of a continuous system on a Poincaré section under impulse forcing. Use of short impulses allows one to linearize the system and calculate the dependence of the magnitude of the map shift on impulse amplitude, which is necessary for control. The technique of map shift does not require knowledge of the model of controlled system, as, for example, in Ref. [21], and does not demand calculation of eigenvalues of the matrix of linearized map, as in the OGY methods.

Similarly, impulse control of chaos may be realized for variation of *system* parameters.

Acknowledgement

This research has been supported in part by the Russian Foundation for Basic Research (Projects 96–02–18041, 96–02–16559, and 97–02–1752), by The Program of Support of Leading Scientific Schools of the Russian Federation (Grant 96–02–96593), as well as by the US National Science Foundation (G.V.O.).

References

[1] A.J. Lichtenberg, M.A. Lieberman, Regular and Stochastic Motion (Springer, New York, 1983).
[2] H.G. Schuster, Deterministic Chaos: An Introduction, 2nd edition (VCH, Weinheim, 1988).
[3] J. Guckenheimer, P. Holmes, Nonlinear Oscillations, Dynamical Systems and Bifurcations of Vector Fields (Springer, New York, 1983).
[4] G. Chen, X. Dong, Int. J. Bifurcation and Chaos 3 (1993) 1363.
[5] G. Hu, Z. Qu, K. He, Int. J. of Bifurcation and Chaos 5 (1995) 901.
[6] M.J. Ogorzalek, IEEE Trans. Circuits and Systems – I: Fundamental Theory and Applications 40 (1993) 700.
[7] E. Ott, C. Grebogi, J.A. Yorke, Phys. Rev. Lett 64 (1990) 1196.
[8] T. Shinbrot, C. Grebogi, E. Ott, J.A. Yorke, Nature, 363 (1993) 411.
[9] Z. Galias, C.A. Murphy, M.P. Kennedy, M.J. Ogorzalek, Proc. IEEE Int. Symp. on Circuits and Systems, ISCAS'96, Atlanta 3 (1996) 120.
[10] S. Rajasekar, M. Lakshmanan, Int. J. of Bifurcation and Chaos 2 (1992) 201.
[11] S. Rajasekar, Phys. Rev. E 51 (1995) 775.
[12] Y. Braiman, I. Goldhirsh, Phys. Rev. Lett. 66 (1991) 2545.
[13] T. Kapitaniak, L. Kocarev, L.O. Chua, Int. J. of Bifurcation and Chaos 3 (1993) 459.
[14] A. Yu. Loskutov, J. Phys. A: Math. Gen. 26 (1993) 4581.
[15] B.A. Huberman, E. Lumer, IEEE Trans. Circuits and Systems 37 (1990) 547.
[16] V. Petrov, M.F. Crowley, K. Showalter, Int. J. of Bifurcation and Chaos 4 (1994) 1311.
[17] A.K. Kozlov, V.D. Shalfeev, L.O. Chua, Int. J. Bifurcation and Chaos 6 (1996) 569.
[18] N.A. Magnitsky, Dokl. Acad. Nauk 351 (1996) 175 [in Russian].
[19] G. Osipov, L. Glatz, H. Troger, Chaos, Solitons & Fractals, 9 (1998) 307.
[20] A.K. Kozlov, G.V. Osipov, V.D. Shalfeev, Vestnik Nizhegorodskogo Univ. 1 (1996) 113 [in Russian].
[21] T.Yang, C.-M. Yang, L.-B. Yang, Phys. Lett. A 232 (1997) 356.
[22] T. Yang, L.O. Chua, Int. J. of Bifurcation and Chaos 7 (1997) 654.
[23] S. Parthasarathy, S. Sinha, Phys. Rev. E 51 (1995) 6239.
[24] L.O. Chua, Archiv für Elektronik und Übertragungstechnik 46 (1992) 250.
[25] A.L. Fradkov, A. Yu. Pogromsky, IEEE Trans. Circuits and Systems–I 43 (1996) 907-913.
[26] K.G. Kiveleva, L.A. Fraiman, Applied Nonlinear Dynamics 2 (1994) 27 [in Russian].